COMPREHENSIVE STUDY OF DIFFERENT PECVD-DEPOSITION METHODS FOR DEPOSITION OF THIN INTRINSIC AMORPHOUS SILICON FOR HETEROJUNCTION SOLAR CELLS

D. Pysch, M. Bivour, K. Zimmermann, C. Schetter, M.Hermle, S. W. Glunz

Fraunhofer Institute for Solar Energy Systems, Heidenhofstr. 2, D-79110 Freiburg, Germany
Phone: +49-761-4588-5287; Fax: +49-761-4588-9250; email: damian.pysch@ise.fraunhofer.de

ABSTRACT: This work tackles the question whether a soft PECVD-deposition of intrinsic, hydrogenised, amorphous silicon (a-Si:H(i)) is really supportive for the passivation quality of the heterojunction interface between a crystalline wafer and the a-Si:H(i)-layer itself. Two PECVD-deposition methods are under investigation: i) parallel plate 13.5 MHz deposition chamber (PP-13.5 MHz), and ii) an inductively coupled plasma deposition chamber (ICP). The time dependent degradation and the thickness dependence of the passivation quality of the a-Si:H(i)-layers are discussed as an important fact to note, when the work aims to compare different a-Si:H(i)-layer deposition techniques and/or deposition parameter sets. The two different PECVD a-Si:H(i) deposition techniques are optimized and compared with the goal to find the highest possible passivation quality while reducing the layer thickness below 10 nm.
Keywords: PECVD-deposition, heterojunction solar cells, amorphous silicon, passivation

1 INTRDUCTION

Silicon Heterojunction solar cells (SHJ-SC) are well known as high voltage and high efficient silicon solar cells. Besides the fact of a high efficiency potential, there are other essential advantages of this solar cell concept. All process steps can be accomplished below 250°C and the whole process is applicable to wafers with a thickness below 100 µm. Such very thin solar cells are still able to perform with efficiencies up to 21% [1].

The best results for HJ-SC so far were achieved on n-type monocrystalline silicon wafers with a thin intrinsic amorphous silicon layer a-Si:H(i) deposited by plasma enhanced chemical vapour deposition (PECVD) on both the front and the rear-side interface followed by a doped amorphous layer. Voltages well above 700 mV and efficiencies above 22% were only reported for SHJ-SC with a thin intrinsic layer [2]. Thus, the quality of this layer, as well as the interface [3, 4], are assumed to be the key-features to achieve exceptionally good performance.

S. Taira et al [2] emphasise that a good surface clean in combination with a soft plasma a-Si:H-layer deposition is crucial for good interface passivation and thus a high open-circuit voltage V_{oc}. In order to produce a high efficiency heterojunction silicon solar cell, two physical demands need to be satisfied. Firstly, a very low defect density at the interface should be assured [5, 6] (generally realised by wet-chemical processes). The cleaning should guarantee a good surface cleaning and smoothing (in the sub-nanometer range)[7]. Secondly, a very low defect density in the first atom layers of the intrinsic, hydrogenized amorphous silicon a-Si:H(i) is assumed to be important.

With the intention of assuring that the optimised wet-chemical surface preparation does not suffer during the ignition of the plasma and the deposition of the first atom layers, an extremely soft deposition technique of the radicals is required. The stress that is created due to the acceleration of the charged particles in the plasma needs to be minimized. The PECVD-deposition technique predominantly used for deposition of intrinsic amorphous hydrogenated silicon a-Si(i):H for passivation or for HJ-SC is the standard parallel plate PECVD setup with a excitation frequency of 13.56 MHz (PP-13.5 MHz-plasma).

In this work we are going to investigate three different PECVD-deposition methods in two different deposition chambers regarding the growth of the best very thin and high quality a-Si:H(i)-layer. In the first chamber a standard and well known 13.56 MHz (RF) parallel plate setup with a variable distance between the electrodes is used. In the second chamber an inductively coupled PECVD-deposition technique (ICP) can be used in two ways: i) with the wafer very near to the actual plasma source (direct-ICP) and the wafer quite far away form the plasma (remote-ICP). An ICP-deposition is known to create low damage plasma with a very narrow distributed and low kinetic energy of the charged particles in the plasma [8].

2 EXPERIMENTAL

The a-Si:H(i)-layers were deposited on flat 1 Ω cm FZ, n-type-wafers. All wafers were cleaned wet chemically by a chemical oxidation of the surface in HNO_3, followed by a removal of the oxide in a 1% HF-solution. After the cleaning step the wafers were placed directly in the deposition chamber or held in an inert environment until the actual deposition took place. The passivation quality of the layer was investigated by lifetime measurements with a Sinton Consulting WCT-100 **Q**uasi-**S**teady-**S**tate **P**hoto **C**onductance (QSSPC) system [9], operated in the so-called generalized as well as in the transient mode[10].

The a-Si(i):H-layer thickness was determined by spectroscopic ellipsometry. All measurements shown here were performed using a J.A. Woolam C. VASE rotating analyzer ellipsometer. The angle of incidence was 70° and a Tauc-Lorentz-model was used to fit the data [11].

All a-Si:H(i)-layer depositions were processed on a Oxford-PECVD-Cluster 100 Pro system, consisting of a load lock, a transfer chamber, and the two PECVD deposition chambers. The first deposition chamber works with a standard parallel plate (PP) 13.5 MHz PECVD technology. In the second chamber, the a-Si:H(i)-layers

are deposited by an inductively coupled plasma (ICP-PECVD). The main plasma is created in a tube which is placed in the center of a coil which is connected to a power generator. The ICP-power-generator is also driven by a 13.5 MHz frequency. This arrangement allows us to decouple the place where the plasma is created from the place where the deposition takes place. Since we are able to vary the sample table height, we are able to decrease the interaction between the ICP-Plasma (especially the charged and high energy particles) and the lifetime sample. Additionally, we are able to apply a RF-power between the upper ICP-source electrode and the sample table, in order to influence the plasma strike properties and the homogeneity of the deposited a-Si:H(i)-layer.

3 THICKNESS DEPENDENCE AND DEGRADATION OF LIFETIME SAMPLES PASSIVATED WITH a-Si:H(i)

3.1 Time dependent degradation of the passivation quality of a-Si:H(i)

We observed that all processed samples independent of the PECVD-method, exhibited a time dependent degradation of the minority carrier lifetime (see Figure 1). In order to guarantee a good comparison between the different samples it is very important to measure all samples at a distinctive time after the a-Si:H(i) deposition stopped. In our experience a good and reproducible measurement point is 10 min after the plasma deposition is finished. The slope of the degradation is influenced by the a-Si:H-layer thickness. Figure 1 shows that the degradation is much stronger for a sample with an a-Si:H-layer thickness below 10 nm, compared with an above 100 nm sample.

One possible explanation of the thickness dependence of time dependent degradation can be that the further the interface between a-Si:H(i) and the environment diverges from the actual HJ-interface the more stable is the passivation quality. This means that the interface region between c-Si and a-Si:H(i) is influenced strongly regarding the stability for a-Si:H(i)-layers below 100 nm. However, since a fully processed HJ-solar cell consists of an additional a-Si:H(p^+)- and ITO-layer, we end up with a total thickness of the stacked layer in the 100 nm region. Thus, we assume that the degradation process is significantly less strong for the 5nm a-Si:H(i) layer in a fully processed HJ-solar cell. Furthermore, M. Hofmann et al. showed that an additional capping-layer on top the a-SI:H(i)-layer can improve their stability [12]

A simple annealing step on a hot plate at 250°C for 10 min in a lab environment recovers the samples to the assumed initial lifetime value directly after the deposition. Some samples even improve their passivation quality. However the same kind of degradation is observed after the annealing step.

The degradation mechanism seems not to be explainable with effusion of hydrogen out of the sample, since the annealing recovery and degradation cycle can be repeated several times without any changes. If the sample is stored in the dark between the measurements, the degradation slope is much smaller. Thus the degradation process might be explained by light induced changes at or very near to the actual HJ-interface. Similar observations have already been published by H. Plagwitz et al. [13].

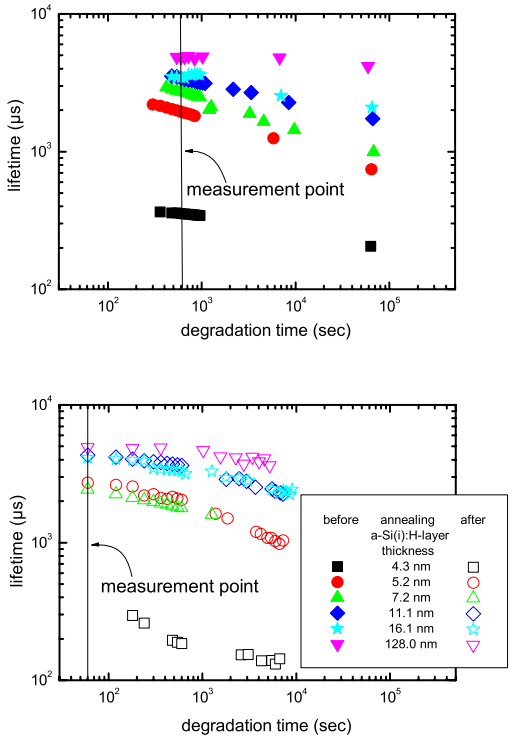

Figure 1: Time dependent degradation of the minority carrier lifetime of 1 Ω cm, n-type, FZ-wafer passivated with different a-Si:H(i)-layer thicknesses. The upper graph shows the measurement directly after deposition and the bottom graph shows the measurements after an additional annealing step. The vertical lines indicate the suggested measurement point to guarantee a good comparison of the samples.

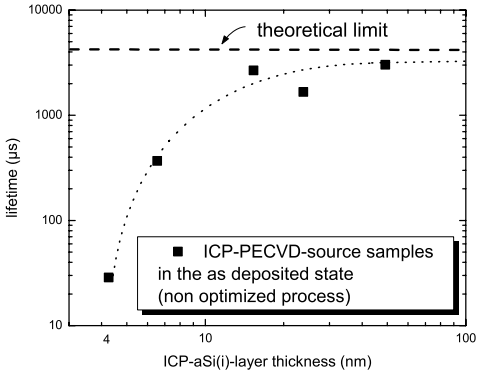

Figure 2: Dependence of the minority carrier lifetime on the a-SiH(i)-layer thickness. All samples have been grown by the ICP-PECVD-technique with a non-optimized process. The theoretical limit is calculated by the Auger-model based on Ref. [14]

3.2 Thickness dependence of a-Si:H(i)-layer passivation

To get a first impression of the dependence of the a-Si:H(i)-layer thickness on the passivation quality we established a process which shows good performance for a Si:H(i)-layer thickness of more than 15 nm (see Figure 2).

However, once the Si:H(i)-layer thickness sinks

below 10 nm we observed a strong decrease in the measured lifetime. Since we are aiming for a good passivation quality of the Si:H(i)-layer thickness below 10 nm, we conducted all further experiment and process variation in the ICP- and PP-13.5 MHz-PECVD-deposition chamber with lifetime samples passivated with a Si:H(i)-layer thickness between 8 and 10 nm to guarantee a good comparability.

4 OPTIMIZATION OF PECVD-DEPOSITION METHODS FOR PASSIVATION WITH THIN INTRINSIC a-Si:H-LAYERS

In this chapter we will present our results of a statistical design of experiment (DOE) for the ICP-PECVD-chamber in detail and for the PP-13.5 MHz chamber, only the most important conclusions. All lifetime samples have been produced on 1 Ω cm, n-type, FZ material, with a wafer thickness of 200-220 µm. The deposited a-Si:H(i)-layer thickness was aimed to be in the range between 8 and 10 nm (see Table I). Lifetime measurements were taken 10 min after the deposition and 1 min after the annealing step.

Table I gives an overview of the parameters that were varied within the statistical DOE for each PECVD-chamber. Also shown in the last column of Table I is the average a-Si:H-layer thickness measured for the ICP-chamber samples 8.1 +/- 3.5 nm (81 samples) and the PP-13.5 MHz 10.0 +/- 3.1 nm (56 samples). Each parameter has been varied in three values (see Figure 5).

Table I: Overview of the parameters that were varied within the statistical design of experiments for the ICP-(81 samples) and the parallel plate 13.5 MHz PECVD-chamber (56 samples). We attempted to keep the a-Si:H(i)-layer thickness around 10 nm as well as keep the thickness variation as low as possible, in order to guarantee a good comparability. (X) Parameter has been varied on three different values, (-) no parameter variation.

PECVD-methods	Power	Pressure	Table height	Tempera-ture	SiH_4-flow	Ar to total Gas-flow	H_2-flow	RF-ICP-power	Layer thickness
ICP	X	X	X	X	X	X	X	X	8.1 +/- 3.5 nm
PP-13.5 MHz	X	X	X	X	X	-	X	-	10.0 +/- 3.1 nm

4.1 ICP-PECVD a-Si:H(i) deposition optimization

Figure 3 shows the Pareto-diagram of the lifetime data measured 10 min after the deposition for all 81 samples created with the ICP-PECVD- technique.

The Pareto-diagram gives us information regarding which parameter has the most significant influence on the measured lifetime. Plotted are the different parameters that have been varied (ordinate) over their effect on the lifetime (abscissa) in normalized values. In the evaluation of the data, linear (L) as well as quadratic (Q) effects of the parameters are allowed. Furthermore, linear interconnections between two parameters are also taken into account. Positive values in the Pareto diagram mean that the highest value leads to the best performance and vice versa for negative values (for a linear (L) approximation). For a quadratic approximation, the sign of the value tells us which curvature the quadratic-fit-function has (see also Figure 5).

It can be seen that the variation of the SiH_4-flow and the ICP-power has the strongest influence on the a-Si:H(i)-layer and hence on the lifetime. Based on the Pareto-diagram, we can conclude that with the: 1) highest SiH4-flow, ii) lowest ICP-power, iii) lowest table height, and iv) lowest pressure we can get the best passivation for an a-Si:H(i)-layer with a thickness below 10 nm.

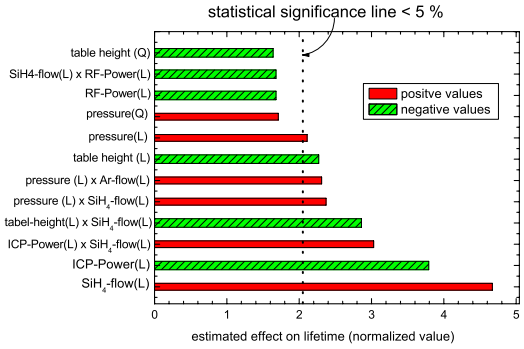

Figure 3: Pareto-diagram presenting the significant influences of the varied parameter within the statistical parameter variation of the ICP-PECVD-technique on the measured lifetime values. On the ordinate the varied parameter and the interconnection between them are listed. On the abscissa their estimated effect on the lifetime in normalized values is shown. The values above the statistical significance line have a probability of less than 5% that the shown effect occurred randomly.

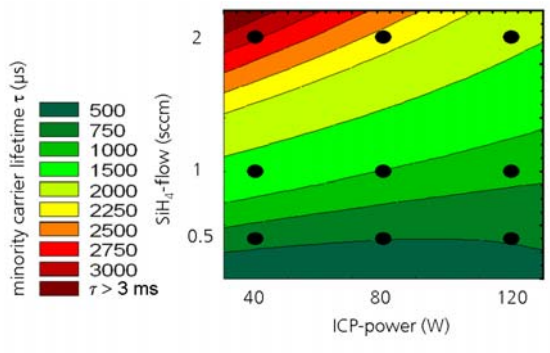

Figure 4: Contour plot of the ICP-PECVD-parameter (ICP-power and SiH_4-flow) with highest influence on the lifetime. It is obvious that the lower the ICP-power and the higher the SiH4-gass flow is chosen the higher the lifetime becomes.

The strong and clear interconnection between the SiH_4-flow and the ICP-power is also shown in Figure 4. It can be seen that the conclusions of the Pareto-diagram completely agree with the contour plot. At this point we can already conclude that we need to minimize the ICP-power and the table height. Both statements tend to a soft and remote a-Si:H(i) deposition regime. Thus we can already deduce that the motivation of this work, to analyze whether a soft PECVD deposition has a positive influence on the passivation quality of ultra thin a-Si:H(i)-passivation layers, seems to be correct for the ICP-PECVD-chamber.

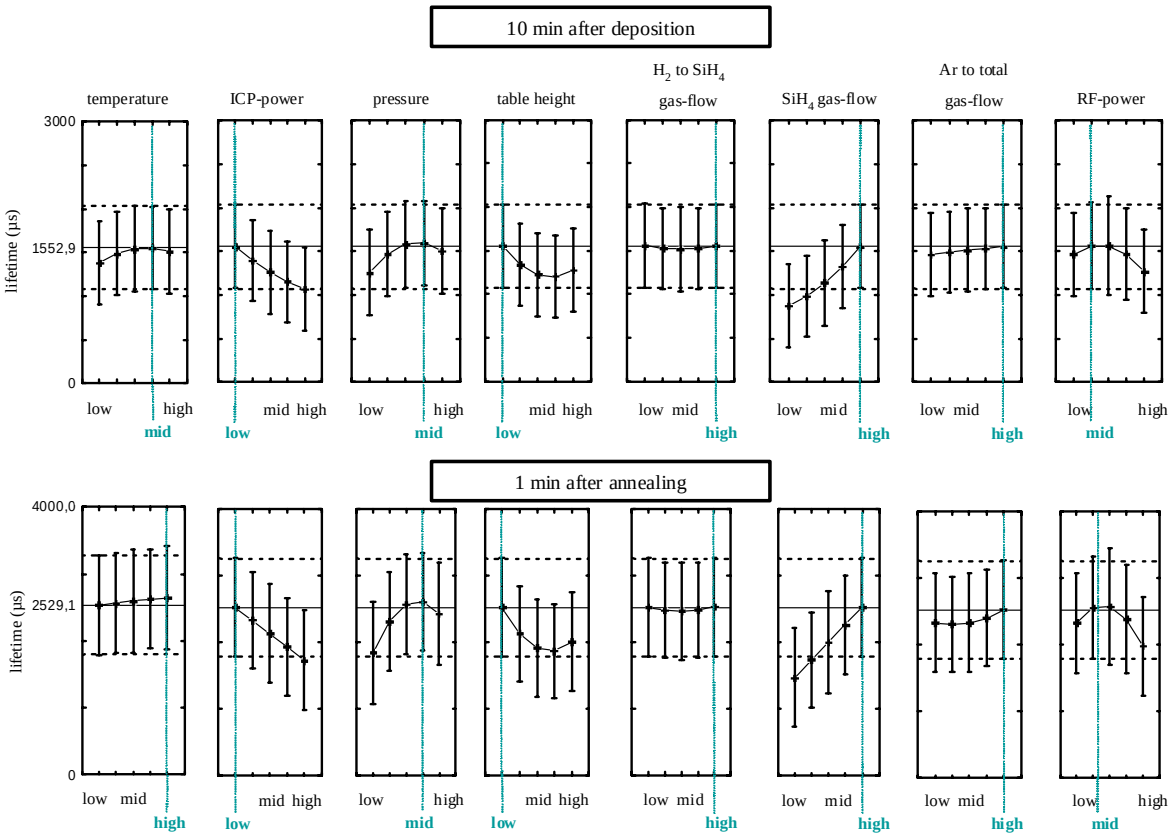

Figure 5: Results of the fit function to the actual measured lifetime data within the statistical design of experiments for the ICP-PECVD- technique. The error bar represents the accordance between the fit-function and the measured lifetime data. The parameter-region which allows a very good passivation is shifted below the other regions (marked in green, colored version). The vertical dotted lines represent the error bar of the best parameters. The upper graphs show the results directly after deposition (measurement point 10 min) and the bottom graphs show the gradients of the lifetime for each parameter variation after a 10 min annealing at 250°C on a hot plate in a lab environment (measurement point 1 min).

Figure 5 shows the results of the fit function to the actual measured lifetime data in greater detail. All lifetime data has been acquired within the statistical design of experiments, processed with the ICP-PECVD-technique. It can be seen very clearly that e.g. the SiH_4-flow has the clearest trend and the highest SiH_4-flow allows for the best passivation, as already concluded from Figure 3. The error bars represent the accordance between the fit-function and the measured lifetime data. At this point we can also find the best values for the parameters which are still open: i) temperature, ii) H_2-to SiH_4-ratio, iii) Ar- to total gas-flow, and iv) RF-power. The parameter regions which allow a very good passivation are shifted below the other values (marked in green, colored version). The vertical doted lines represent the error bar of the best parameters.

The upper graphs in Figure 5 show the results measured directly after deposition (10 min) and the bottom graphs show the gradients of the lifetime for each parameter variation after a 10 min annealing at 250°C on a hot plate in a lab environment. The measurement has been taken 1 min after the annealing step. Basically, the optimum process stay unchanged, however the lifetime increases after the annealing step by approximately 1 ms to a value of 2.5 ms (for the best approximated fit-function). Based on the measurement of Figure 1, we believe that it might be possible to keep the improved level after annealing for a final front side layer stack system including the doped amorphous silicon and the transparent conductive oxide with a total thickness in the range of 100 nm [12].

4.2 PP-13.5MHz-PECVD

For the PP-13.5 MHz-PECVD-chamber, the trends are not as clear as for the ICP-PECV-chamber. The Pareto-diagram of the varied parameters plotted versus their effect on the measured lifetime (normalized) shows only a significant trend for the applied power, the interconnection between the power and the pressure, and the table height (see Figure 6). All other parameters can be deduced based on a graph as shown in Figure 5 (not shown here).

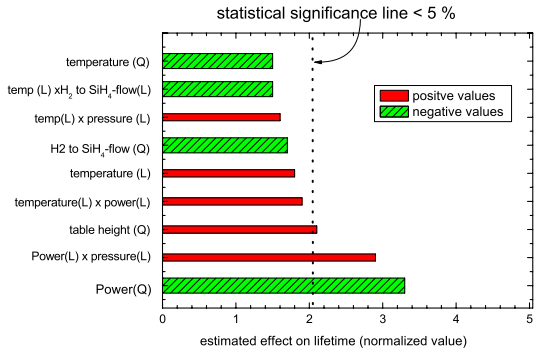

Figure 6: Pareto-diagram presenting the significant influences of the varied parameters within the statistical parameter variation of the PP-13.5 MHz-PECVD-technique on the measured lifetime values. On the ordinate the varied parameter and the interconnection between them are listed. On the abscissa their estimated effect on the lifetime in normalized values is shown. The values above the statistical significance line have a probability of less than 5% that the shown effect occurred randomly.

Furthermore, the evaluation of the lifetime samples after deposition and directly after annealing (250°C for 10 min on a hot plate) processed in the PP-13.5 MHz chamber samples show strong differences. In Figure 7 an example is shown of how the trends can change after a post-deposition annealing. The optimum power changes form 100 W before to 10 W, and the best pressure changes from 500 to 200 mTorr after an annealing step. Also the temperature changes from the highest temperature used, 355°C, to the lowest temperature, 290°C.

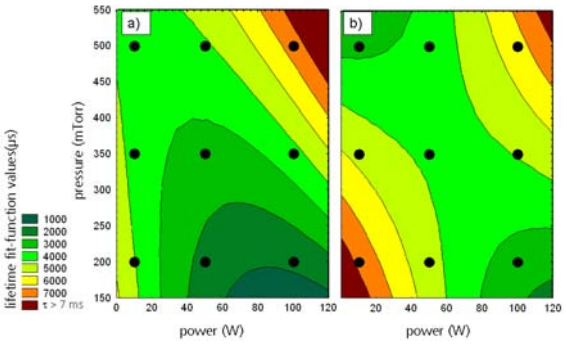

Figure 7: Contour plot of the PP-13.5 MHz-PECVD-parameter with the highest influence on the lifetime (pressure and power). Contour plot a) shows the dependence of the power and the pressure measured 10 min after deposition. Contour plot b) shows the same parameter, however after an annealing step (measured 1min after annealing).

In conclusion, the statistical design of experiments we accomplished with 56 lifetime samples for the PP-13.5 MHz-chamber, does not allow as many definite conclusions as for the ICP-PECVD-chamber. We observed a difference between the optimum deposition parameter in the as deposited- compared to the annealed-state for the following parameter: temperature, power, and pressure. However, the suggested best process after the annealing shows a clear trend to soft plasma deposition as well (reduction of power, pressure, and temperature).

5 COMPARISON OF THE THICKNESS DEPENDENCE OF THE OPTIMIZED THIN INTINSIC a-Si:H-LAYER

In this chapter we finally compare the optimized processes in regard to their passivation quality for a-Si:H(i)-layer thicknesses below 10 nm. Figure 8 shows the lifetime data measured 10 min after deposition and 1 min after an annealing step, plotted versus the a-Si:H(i)-layer thickness. We see a strong improvement from the non-optimized (see also Figure 2) to the new and optimized process for the ICP-PECVD-chamber. A comparison between the optimized Si:H(i)-layers of the ICP- and the PP_13.5 MHz chamber reveals that the layers are showing a identical performance down to a a-Si:H(i)-layer thickness of only 8 nm. However, below 8nm the very soft ICP-PECVD provides a better passivation quality.

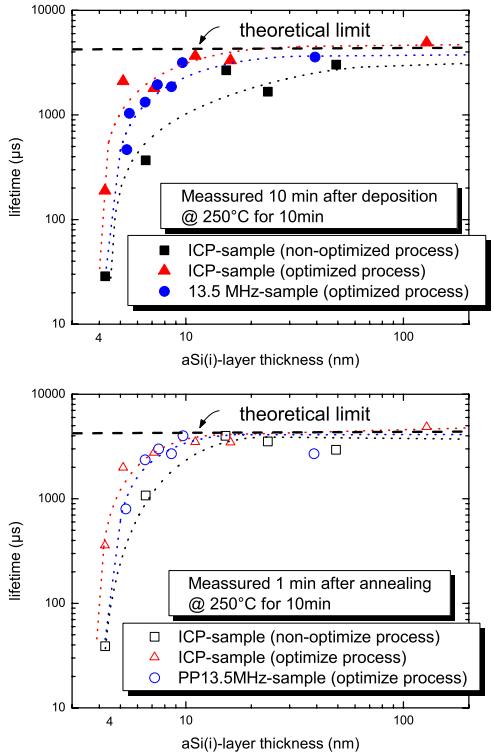

Figure 8: Comparison of the thickness dependence of a non-optimized ICP-PECVD process with a optimized processes of the ICP-PECVD- and the PP-13.5 MHz-PECVD a-Si:H(i) passivated lifetime samples. The upper graph shows data measured 10 min after the deposition, and the bottom graph shows data measured 1 min after an annealing step. Dotted lines are guides to the eye.

6 CONCLUSION

In this work we have investigated the influence of different plasma conditions on the passivation quality of a-Si:H-layers. The time- and a-Si:H-layer thickness-dependent degradation of the passivation quality have been presented. This observation led us to the conclusion that it is very important to set up a distinctive measurement point regarding the degradation time after the deposition or an annealing step to be able to compare different samples with another. For a non-optimized deposition process we observed a strong degradation of the lifetime if the passivation layer thickness is reduced below 10 nm. A statistical DOE for both the ICP- and the PP-13.5 MHz a-Si:H(i) deposition chamber led us to improved processes. The results of the optimized process for both deposition techniques show a clear trend that the softer the deposition is performed, the better passivation qualities can be obtained for very thin a-Si:H(i) layers below 10 nm. The comparison of the ICP- and the PP-13.5 MHz chamber let us conclude that both deposition techniques allow the creation of very thin and anyhow still very good passivating a-Si:H(i) layers. However, the ICP-PECVD-chamber seem to perform even slightly better for a-Si:H(i)-layer thickness below 7 nm.

7 ACKNOWLEDGMENT

The authors would like to thank A. Leimenstoll, F. Schätzle, T. Krishnamurthy, C. Meinhardt for wet-chemical cleaning of the wafer and measurements. This work was funded by the German Federal Ministry for the Environment, Nature Conservation and Nuclear Safety under contract number 0329849A (Th-ETA).

8 REFERENCES

[1] H. Kanno, D. Ide, Y. Tsunomura, S. Taira, T. Baba, Y. Yoshimine, M. Taguchi, T. Kinoshita, H. Sakata, and E. Maruyama, in Proceedings of the 23rd European Photovoltaic Solar Energy Conference, Valencia, Spain, 2008, p. 1136.

[2] S. Taira, Y. Yoshimine, T. Baba, M. Taguchi, H. Kanno, T. Kinoshita, H. Sakata, E. Maruyama, and M. Tanaka, in Proceedings of the 22nd European Photovoltaic Solar Energy Conference Milan, Italy, 2007, p. 932.

[3] H. Angermann, J. Rappich, and C. Klimm, Central European Journal of Physics 7 (2009) 363.

[4] H. Angermann, J. Rappich, L. Korte, I. Sieber, E. Conrad, M. Schmidt, K. Hübener, J. Polte, and J. Hauschild, Applied Surface Science 254 (2008) 3615.

[5] D. Pysch, J. Ziegler, J.-P. Becker, D. Suwito, S. Janz, S. W. Glunz, and M. Hermle, Applied Physics Letters 94 (2009) 093510/1.

[6] J.P. Becker, D. Pysch, A. Leimenstoll, M.Hermle, S. Glunz (presented at this conference) (2009)

[7] H. Angermann, W. Henrion, A. Röseler, and M. Rebien, Materials Science and Engineering B73 (2000) 178.

[8] S. J. Schreiber, in Department of Engineering, University of Cambridge, Cambridge, 2001, p. 177.

[9] R. A. Sinton and A. Cuevas, Applied Physics Letters 69 (1996) 2510.

[10] H. Nagel, C. Berge, and A. G. Aberle, Journal of Applied Physics 86 (1999) 6218.

[11] A. Richter, J. Benick, and S. W. Glunz, in Proceedings of the 23rd European Photovoltaic Solar Energy Conference, Valencia, Spain, 2008, p. 1724.

[12] M. Hofmann, C. Schmidt, N. Kohn, D. Grambole, J. Rentsch, S. W. Glunz, and R. Preu, in Proceedings of the 22nd European Photovoltaic Solar Energy Conference Milan, Italy, 2007, p. 1528.

[13] H. Plagwitz, B. Terheiden, R. Brendel, Journal of Applied Physics 103, 094506, (2008).

[14] M. J. Kerr and A. Cuevas, Journal of Applied Physics 91 (2002) 2473.